



Optimization of Ag Micro-Flakes Fabrication for Plasmonics Applications

Final Report
Spring 2024

Mehdi AMOR

Supervisor: Sergejs BOROVIKS
Professor: Olivier J.F. MARTIN

June 25, 2024

Abstract

This report presents the findings aimed at optimizing the synthesis of monocrystalline silver flakes for enhanced plasmonic applications. The study investigates the influence of various synthesis parameters, including solute concentration, temperature variations, and reaction time, on the morphology and size of silver flakes produced via a chemical reduction process. The experiments demonstrated that while higher solute concentrations generally promote flake growth, there is a critical concentration beyond which the average flake size plateaus, and temperature variations showed that room temperature conditions are most conducive to achieving optimal flake size and quality. Additionally, the study explored advanced strategies such as supersaturation control, the use of stabilizing agents, and seeded growth techniques to refine flake characteristics and control their growth kinetics more precisely. The results are for some parts promising. The optimized parameters and methods identified in this study offer interesting directions for future research and application in materials chemical growth related fields.

Contents

Abstract	3
1 Introduction	4
1.1 Literature review	4
2 Methodology	5
2.1 Materials, Reagents and Experimental Setup	5
2.2 Colloidal Growth Theory	6
2.3 Variables Testing	7
2.3.1 Concentration Variation	7
2.3.2 Temperature Variation	8
2.3.3 Reaction Time Variation	8
2.4 Additional Optimization Strategies	8
2.4.1 Supersaturation control	8
2.4.2 Use of Stabilizing Agents	9
2.4.3 Seeded Growth	10
2.5 Characterization Methods	10
3 Results	10
3.1 Concentration Variation	11
3.2 Reaction Time Variation	12
3.3 Temperature Variation	12
3.4 Supersaturation Control	13
3.5 Surface Stabilizing Agents and Seeded Growth	14
4 Conclusion	15
5 Appendices	17

1 Introduction

Plasmonics, a subfield of nano-optics focusing on light-matter interactions at metal surfaces, has expanded into various domains such as microscopy, sensing, and optical communications. Despite its potential, the performance of plasmonic systems is significantly hindered by Ohmic losses at optical frequencies, particularly in noble metals. Addressing these losses is crucial for advancing the field and can be achieved by employing crystalline materials that exhibit lower roughness and are free from structural defects.

Monocrystalline silver flakes, synthesized chemically, present a promising solution due to their potential for reduced losses and enhanced plasmonic properties. The NAM laboratory is currently leading research in synthesizing noble metal flakes colloids and developing nanopatterning techniques. This project aims to contribute to these efforts by focusing on the chemical synthesis of silver flakes with large aspect ratios, characterizing these nanostructures, to further study surface plasmon polariton (SPP) propagation on them.

The objectives of this project include familiarizing with colloidal synthesis methods and theory, optimizing synthesis parameters for fabricating monocrystalline silver flakes, and sample characterization.

1.1 Literature review

The exploration of plasmonic materials has intensified in recent years. Silver has emerged as a leading material in this field due to its superior plasmonic properties, such as the lowest intrinsic loss at optical frequencies [7]. This literature review synthesizes findings from four key papers, highlighting advances in the synthesis, characterization, and application of silver microstructures in plasmonics.

Lyutov et al. (2014) [2] and Zhang et al. (2019) [10] describe a straightforward one-step synthesis method for producing large single-crystalline silver hexagonal microplates. The latter are created by reducing silver nitrate in an aqueous solution with 4-(methylamino)phenol sulfate. The resulting microplates, characterized using techniques like scanning electron microscopy (SEM) and transmission electron microscopy (TEM), exhibit high crystallinity and sharp edges, and have lateral dimensions up to tens of microns (20 - 50 μm) and thicknesses between 100 and 300 nm.

Furthermore, Wang et al. (2015) [6] reported the growth of giant colloidal silver crystals with millimeter-scale lateral sizes and thicknesses of tens of microns. Using a platinum-catalyzed, ammonium hydroxide-controlled polyol reduction method, they synthesized single-crystalline Ag plates. The process involved increasing the concentration of ammonium hydroxide to control the reaction rate, allowing the formation of large $\text{Ag}(\text{NH}_3)_n^+$ complexes and significantly slowing down the reduction rate. The extended reaction time, spanning several days, resulted in the formation of ultrasmooth, macroscopic-sized silver crystals. These giant crystals exhibit enhanced plasmonic properties, with SPP propagation lengths exceeding 100 μm in the red wavelength region.

2 Methodology

2.1 Materials, Reagents and Experimental Setup

The decision to use Silver Nitrate and Metol for this project stems from their previous use in growing silver flakes, yielding promising results [2], [10]. However, there hasn't been any research on optimizing the growth using these two specific reagents. The advantage lies in the simplicity of the reaction, meaning using primarily two reagents only, that react quickly, making it easier to conduct optimization experiments and identify what works best. This contrasts with other methods, like the one discussed in Wang et al. [6], which produces larger flakes but involve complex recipes that are challenging to replicate. Therefore, by focusing on Silver Nitrate and Metol, we aim to streamline the process and pinpoint the most effective conditions for producing silver flakes.

Here is a concise description of the reaction steps:

1) Metol has a hydroxyl group (-OH) that will react with a hydroxide ion (OH^-) present in the solvent solution, producing H_2O and forming an ion. **2)** When silver nitrate is dissolved in deionized (DI) water, it dissociates completely into silver ions (Ag^+) and nitrate ions (NO_3^-) due to its high solubility in water. The metol ion then donates an electron to a silver ion, reducing it to metallic silver (Ag^0). As it gets oxidized, the ion's oxygen loses one valence electron. **3)** In order to stabilize, the molecule rearranges to form a quinone-like structure (oxygen double bonds with carbon) **4)** It will further reduce another silver ion and finally react with a hydroxide ion to produce the final stable product, 4-(methyl-amino)cyclohexa-2,5-dienone.

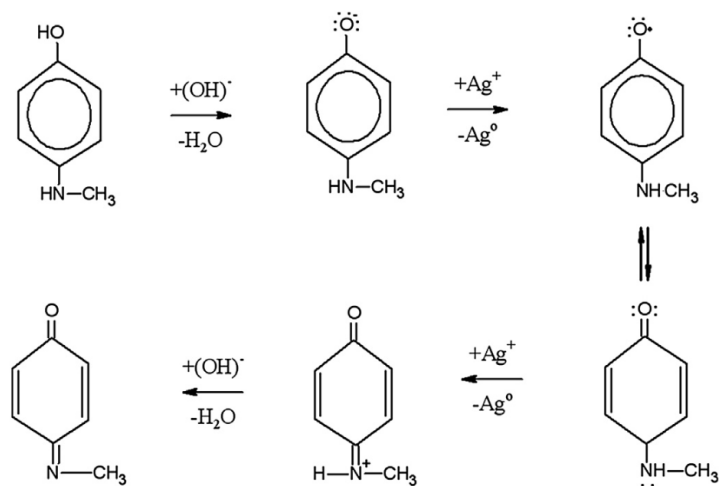


Figure 1: Mechanism of reduction of Silver Nitrate aqueous solution with Metol [2]

For the experimental setup, plastic containers were used to mix the solutions. To ensure proper dilution, an automatic stirrer was employed. Temperature regulation was achieved using a hotplate to heat the solutions, while a centrifuge equipped with temperature control was used for cooling (recipients were placed in the centrifuge without activating the centrifuge itself).

2.2 Colloidal Growth Theory

The colloidal growth of nanocrystals, particularly in two-dimensional forms, has garnered vast attention compared to cleanroom processes. It is cheaper, allows high surface areas, and avoids the forming of semicontinuous or grainy thin films that lead to more losses. Two major sources, Nasilowski et al. (2016) [3] and Scarabelli et al. (2023) [5], provide comprehensive insights into the theories and mechanisms behind the growth of colloidal nanocrystals.

This growth follows the classical nucleation theory introduced by LaMer. This theory involves two main stages: nucleation and growth. Nucleation occurs when the concentration of precursors in a solution exceeds a critical supersaturation point, leading to the formation of small, stable nuclei. Growth subsequently takes place as additional monomers deposit onto these nuclei.

Nasilowski et al. explain that the nucleation phase is critical for determining the final size and shape of the nanocrystals. The LaMer model describes a "burst nucleation" process, where a rapid increase in precursor concentration leads to the simultaneous formation of many nuclei. First, the concentration of monomers increases rapidly in the solution rising to a level of supersaturation, denoted as C_s . As the concentration of monomers continues to increase, it eventually reaches a higher concentration, C_{max} , at which the activation energy barrier for nucleation is overcome. The rapid formation of nuclei causes the concentration of monomers to drop sharply as monomers are consumed to form nuclei. Then, nucleation stops because the concentration of monomers has dropped, and it continues to decrease slowly as they are used up in the growth process. No new nuclei form during this phase; only the existing nuclei grow larger, as long as there is no new addition of reactant.

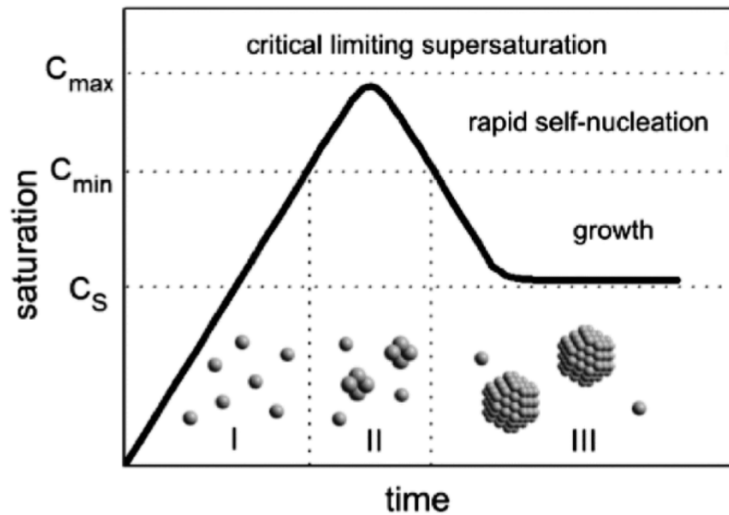


Figure 2: Evolution of the monomer concentration vs time according to LaMer's theory of burst nucleation [3]

The basic idea behind the theory is that a thermodynamic system tends to minimize its Gibbs free energy or increase its entropy. The Gibbs free energy of a spherical cluster can be expressed as follows :

$$\Delta G = -\frac{4}{3}\pi r^3|\Delta G_V| + 4\pi r^2\gamma \quad (1)$$

where r is the radius, $|\Delta G_V|$ is the difference in the Gibbs free energy per unit volume, and γ is the surface energy per unit area, i.e., the energy needed to create a surface of unit area.

The first volume term represents the decrease in Gibbs free energy due to the formation of bonds within the cluster. It is negative, indicating it is a favorable event (energy decreases as volume increases). The second surface term represents the increase in Gibbs free energy due to the creation of a new surface. It is positive, indicating it is an unfavorable event (energy increases with surface area).

The change in the Gibbs free energy due to the formation of a bond between a cluster and a monomer therefore corresponds to a competition between the decrease of the volume energy and the increase of the surface one. Below a certain critical size, corresponding to the critical radius, (calculated by canceling the derivative of Eq. 1) :

$$r_c = \frac{2\gamma}{|\Delta G_V|}$$

the positive surface energy increase is higher, thus pushing the system toward dissolution: growth is unfavorable. Above r_c , the negative volume energy decrease is higher, thus additional atoms will preferentially attach to it, leading to its growth. Smaller particles or nuclei have higher surface energy due to their larger surface-to-volume ratio and when they attach to each other to form larger structures, the overall surface energy of the system is reduced, which is thermodynamically favorable. These equations help understand that there should be careful attention to how much energy is provided to the system, to avoid a nucleation burst where very small particles can be stable, hindering the energy for growth.

Furthermore, as said, the nanoparticle (NP) will grow in such a way to reduce its surface energy, which is the limiting parameter, already present in the nucleation step, which means the shape of a crystal is dictated by the minimization of this energy. Therefore, it is not dictated by the minimum total surface (which is a sphere) but depends strongly on crystalline facets. The final equilibrium shape will be dominated by the facets with the lowest surface energies, hence the anisotropic shape of the silver flakes, which have (111) facets with higher surface energy.

2.3 Variables Testing

The chosen experiments aimed to progress from vague optimization to clearer information and direction. Initially, I attempted to replicate the exact methodology outlined in the Lyutov et al. paper on three separate occasions, but the results consistently yielded minute particles, less than 1 micron in size, rather than the anticipated large flakes. So, I began with basic variables as described beneath, with the idea of increasing growth rate and decreasing nucleation, by slowing the reaction in any way possible, identifying the most conclusive experiments, and develop from there.

2.3.1 Concentration Variation

Concentration plays a pivotal role in energizing the system, by increasing or decreasing collision frequency and enhancing reaction rate, as there are more or less particles per unit volume that can interact with each other. Drawing inspiration from the concentrations used in the

Lyutov paper (2.9mM of Metol and 6mM of AgNO₃), I opted to widen the scope by exploring a concentration range from 0.75mM to 9mM (0.75, 1.45, 2.9, 4.5, 6, 9mM), the increments are 1.5 mM, equivalent to 10 mg/ 40ml. The hypothesis is that lower concentrations will allow for higher growth rates, in case the reaction rate is dependent on the reactants concentrations.

To ensure consistency and comparability across experiments, I standardized the volume to 5ml. If the reaction had failed to reach saturation within this concentration range, I would consider additional concentrations subsequently.

2.3.2 Temperature Variation

Temperature modulation influences the energy input to the system as well, impacting the reaction dynamics by increasing the kinetic energy of molecules, leading to more frequent and more energetic collisions, as well as by affecting the proportion of molecules that have enough energy to overcome the activation energy barrier. For temperature dependant reactions, Arrhenius equation can be used to understand the impact of temperature:

$$k = Ae^{-\frac{E_a}{RT}}$$

where k is the rate constant, A is the pre-exponential factor, E_a is the activation energy, R is the gas constant, T is the temperature in Kelvin.

Temperatures of 1°C, selected as the lowest temperature above freezing point, room temperature ($\sim 20^\circ\text{C}$), and 40°C, representing a higher temperature boundary, were chosen for experimentation. These contrasting temperatures were expected to elucidate any clear trend in reaction kinetics, with the hypothesis again, that lower temperatures will have a positive impact on growth rates.

2.3.3 Reaction Time Variation

The purpose of monitoring the reaction time was to determine when the reaction reaches completion, and to assess whether allowing more time for the flakes to grow leads to further growth or not. If it is the case, the duration before the growth saturates can be determined. For all experiments, I examined the flakes immediately after mixing the reactants and again 10 minutes later to observe any trends.

2.4 Additional Optimization Strategies

After conducting those initial experiments, I proceeded to explore more complex methods commonly used for growing particles and plates in colloidal solutions. I experimented with three techniques: supersaturation control, stabilizing agents, and seeded growth [3], [5].

2.4.1 Supersaturation control

Supersaturation is a state of a solution where the concentration of solute (in this case, monomers or precursor molecules) exceeds the equilibrium solubility. This means the solution contains

more dissolved material than it would under normal circumstances at a given temperature and pressure. It can be achieved by rapidly adding more solute to the solution than can be dissolved at equilibrium, cooling a saturated solution quickly so that solute remains dissolved even though it should precipitate out, or evaporating the solvent from a saturated solution, increasing the concentration of solute. In simpler terms, monitoring supersaturation can allow us to complete the cycle shown in 2 one at a time, and make sure that the concentration of monomers rise gradually, promoting the growth of existing nuclei rather than the formation of many new ones.

For this experiment, I tested various combinations of incremental addition volumes and waiting times between additions. Specifically, I prepared a container with 5 ml of diluted AgNO_3 in DI water, and incrementally added 10 μl , 30 μl , 50 μl , and 100 μl of metol, with waiting times of either 1 minute, 3 minutes, or 5 minutes between each addition, and verified each time the results. It is also important to keep a considerable reaction rate so that the desired dimensions can be obtained within a reasonable period.

2.4.2 Use of Stabilizing Agents

Commonly used toolq in colloidal growth are stabilizing agents, or ligands. Typically, these chemical species serve as capping agents to control the size of spherical particles, used later for applications like plasmonics. These ligands can also preferentially adsorb onto specific facets of crystalline particles like silver, reducing their surface energy and thereby limiting the addition of new particles on top of them, allowing control over the shape of the particles and their surface smoothness, making them more anisotropic and uniform. This can indirectly result in larger particles, as they become thinner, providing more opportunities for the particles to attach to the sides and grow. Ligands can also help minimize self-nucleation rates, as shown in 3.

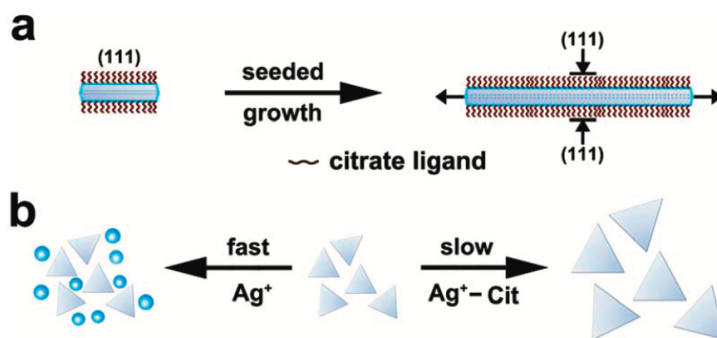


Figure 3: (a) The citrate ions selectively protect the $\{111\}$ facets of Ag nanoplates and only allow lateral overgrowth. (b) Ag - Citrate complexes are used as the precursors, which can effectively slow down the reaction rate and minimize the self-nucleation events [9]

I used two ligands frequently cited in the literature for metallic crystalline growth : Citrate [8], [5], [4] and Halide ions (KCl) [1]. I based my first approach on the ratios used in these studies. Initially, I tried a ratio of 0.7 between the ligand's and the reactants' concentrations, and then experimented with much higher ratios (1:100, 1:1000). The reasons for these specific ratios and their effects will be discussed in the results section.

2.4.3 Seeded Growth

Seeded growth is a method used in the synthesis of nanocrystals where pre-formed "seed" particles are used to promote and control the growth of larger particles [9]. This technique separates the nucleation and growth phases, by creating nanoparticles in a separate initial step that will act as templates or nucleation sites to the newly formed Ag particles, as the surface energy necessary for nucleation is lower at phase boundaries [3]. The reactants can be further added to the solution. By starting with uniform seeds, the resulting particles tend to be more uniform in size and shape, and the likelihood of uncontrolled aggregation is decreased since nucleation sites are limited to the preformed seeds.

This technique is complex in this case, as it requires the seeds to form relatively slowly, unlike in the Metol and AgNO₃ reaction, which is very fast. A slow reaction would allow sufficient time to harvest and use the seeds before they grow larger. If they do, it can defeat the purpose of the experiment, as smaller seeds catalyze more uniform growth from an earlier stage. Larger flakes are more susceptible to contamination, and handling them (e.g., by dropcasting) can lead to their deterioration.

2.5 Characterization Methods

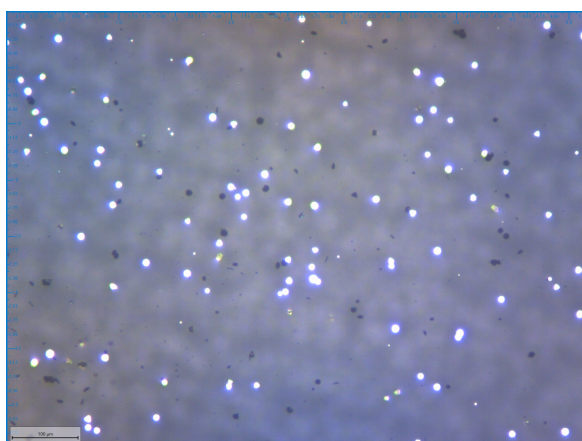
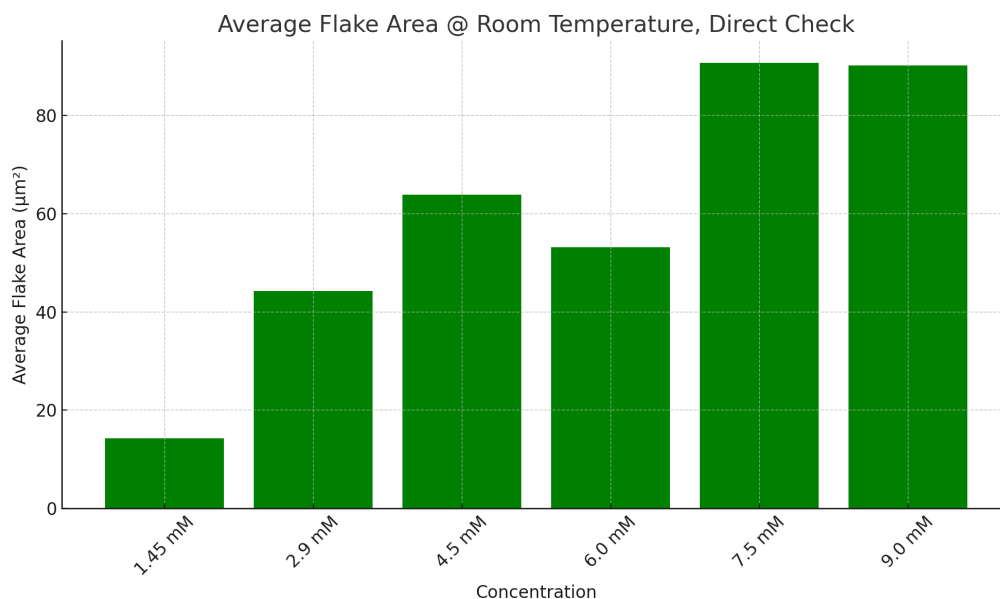
Three features can be considered to determine if the flakes meet the requirements: lateral dimensions, surface smoothness, and contamination by other silver nanoparticles due to aggregation. The easiest way to assess these features is by using the optical microscope available in the NAM lab. Here are the usual steps: grow the flakes, dropcast some of the solution with a pipette between two glass substrates or on a silicon substrate, and examine them under the microscope (after evaporating the excess solvent on a hotplate for the Si substrate).

Moreover, I used the ImageJ Fiji software, which allows for the automatic image detection of particles, and provides a table of the number of flakes along with their respective areas. This is ideal for identifying dimensions, contamination, and growth trends. To characterize the surface in more detail, I used the SEM available at the CMi. I also worked in the cleanrooms to fabricate gridded substrates, which help in better locating the flakes.

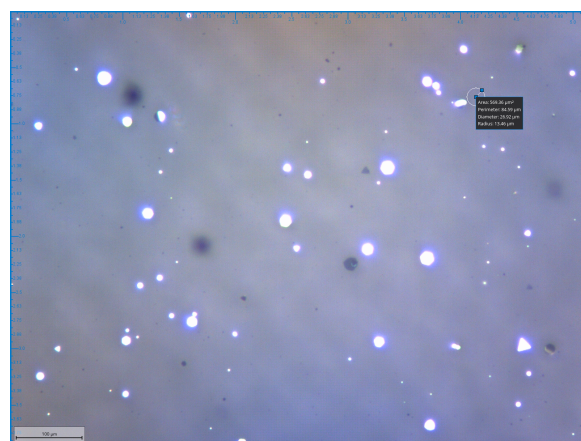
3 Results

The results presented below are based on the statistical analysis of the flakes. Two graphs are included: one is a histogram showing the average number of flakes, offering a quick and broader view of the overall trend. The second one is a fitted Gaussian curve 5, which provides a comparative analysis of the distributions using probability density. This approach normalizes the bins to account for differences in sample sizes, that are very different for each experiment, allowing for a direct comparison of the shapes and spread of the distributions without bias. Each sample consists of two images taken of flakes that represent two random drops of the solution.

3.1 Concentration Variation



(a)

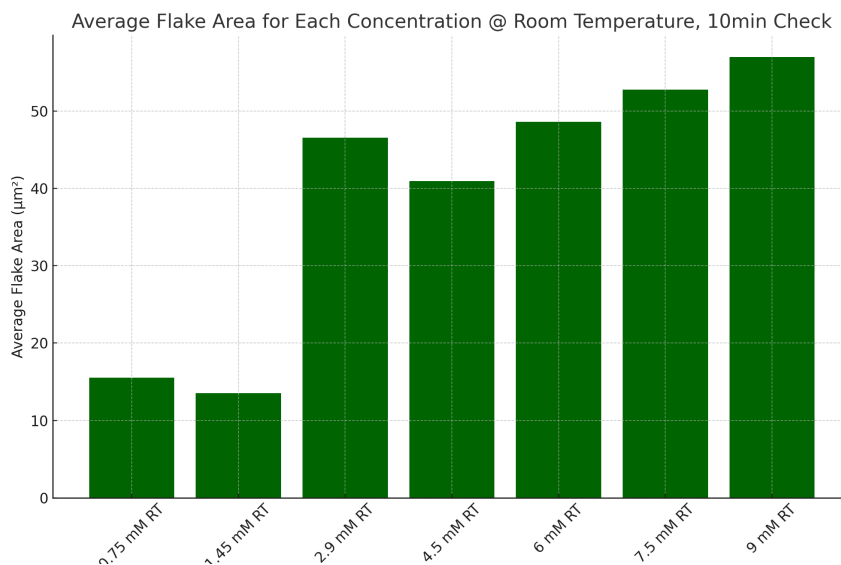


(b)

Figure 4: Samples of two solutions (a) 2.9 mM and (b) 9 mM @ Room Temperature, Direct Check

Based on the observations from the graphs, it is evident that at slightly higher concentrations, the flakes exhibit larger sizes, a distinction that is visually clear in the accompanying images. Specifically, the flakes at 7.5 mM and 9 mM concentrations appear similar, indicating that the saturation of the solution begins around this range. At concentrations up to 15 mM, the flake area showed a tendency to plateau. This supports the hypothesis that higher concentrations initially promote rapid growth, leading to flakes reaching a certain average size. Beyond this point, additional material may contribute to the formation of smaller particles instead of larger flakes. Conversely, lower concentrations do not provide enough material for substantial growth within the same timeframe, resulting in fewer larger flakes observed. Based on this analysis, it can be concluded that a concentration of 9 mM is optimal to initiate further investigations.

3.2 Reaction Time Variation



The experiment aimed to assess whether extending the reaction time would lead to continued or stable growth in flake size. Contrary to expectations, the results showed a decrease in flake area over time. This decrease is likely due to flakes aggregating and settling at the bottom of the container. Consequently, the samples collected for analysis primarily represented flakes that remained suspended in the solution, potentially skewing the observed trend towards smaller flake sizes.

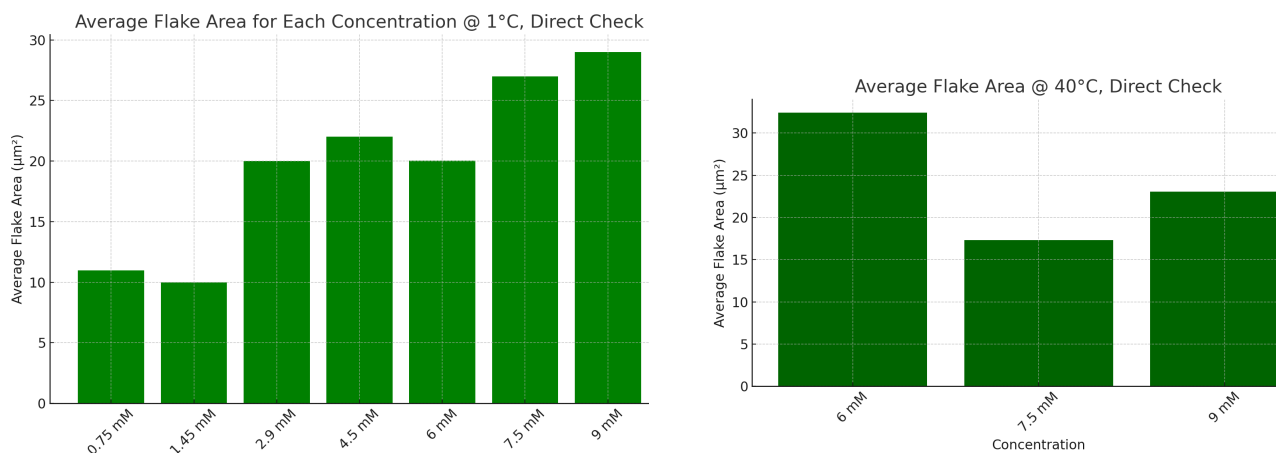
This experiment highlights the importance of gentle stirring to prevent flake aggregation and localized supersaturation. Agitation that is too vigorous can break apart the flakes. Despite attempting to use a magnetic stirrer for consistent mixing, it proved ineffective and particles clumped on the bar. Stirring manually or using an automatic stirrer at very low intensity is advisable to achieve better results. Another technique explored in other studies involves using a substrate directly in the solution to serve as nucleation sites for the formation and growth of flakes. In this experiment, particles predominantly aggregated on the substrate, rendering this approach unsuitable.

3.3 Temperature Variation

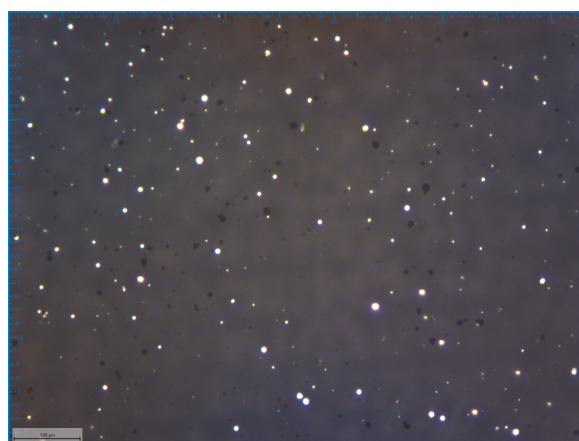
We observe that the size of the flakes does not significantly increase at either 1°C or 40°C (where only three concentrations were tested due to the consistent trends). This phenomenon may be attributed to several factors.

At lower temperatures, the reduced kinetic energy of molecules limits the rate of solute diffusion toward the flake surfaces. Also, lower temperatures slow down chemical reactions and processes, including the nucleation and growth phases of flake formation. Conversely, higher temperatures accelerate molecular movement, increasing the rate of nucleation. While this might suggest favorable conditions for larger flakes, it can result in the formation of numerous small nucleation sites rather than promoting the growth of fewer, larger flakes. Room temperature appears to be the most optimal condition, which is advantageous as it enhances reproducibility.

This observation is consistent with the methodologies of other studies that maintain room temperature reactions.



(a)



(b)

Figure 6: Samples of two solutions (a) 2.9 mM and (b)9 mM at 1°C, direct check

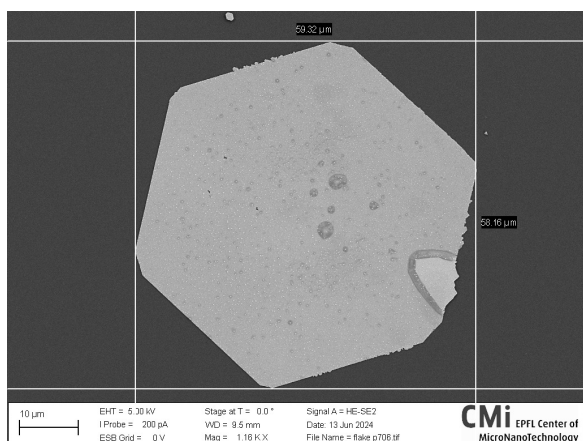
3.4 Supersaturation Control

This variable proved to be highly effective in this experiment, resulting in flakes with significant lateral dimensions. 7a and 8a depict hexagonal flakes measuring approximately 60 µm and 83 µm in diameter, respectively. This was achieved by sequentially adding 10 µl of 9 mM Metol in 5 ml of 9 mM AgNO₃, with two intervals of 5 minutes, followed by additional 50 µl with a 3-minute interval, with constant stirring. The purpose of this concentration strategy was to create a small quantity of nuclei for subsequent attachment, optimizing growth conditions without excessively prolonging the process time. Incrementing with 100ul was too high and precipitated the solution and starting with 10ul or 20ul made the process too slow.

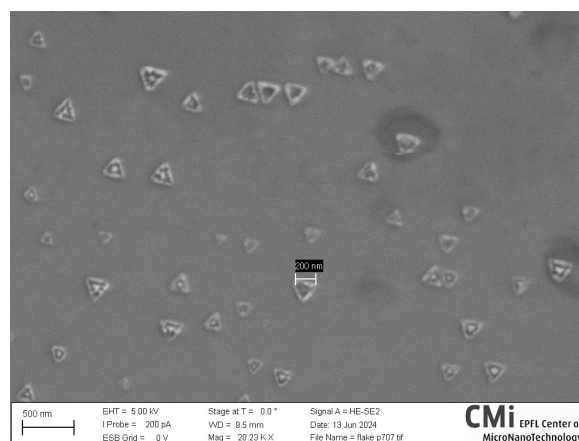
Moreover, the reason behind slowly adding Metol to AgNO₃ and not the opposite, is to ensure that silver ions are uniformly dispersed beforehand. The gradual addition reduces the concentration of silver ions steadily, leading to a controlled nucleation process. In contrast, adding the Silver Nitrite solution dropwise into Metol introduces localized high concentrations

of silver ions near each droplet upon entry. This method can result in uneven nucleation kinetics and potentially smaller flakes or increased aggregation due to fluctuating supersaturation levels.

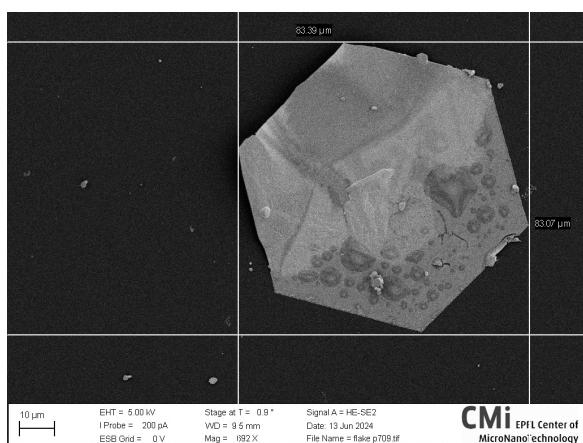
After adding approximately 300 μl of Metol, flakes began to appear, reaching their maximum size at around 800 μl . There were further increases in size, but aggregation also increased, rendering the flakes unsuitable for further manipulation. The results show no juxtaposition or aggregation of flakes on each other (see Figures 8b and 9), but they exhibited small growths on their surface, as seen in 7b, where small nanoparticles of approximately 200 nm side length were observed, which is problematic for SPP propagation. 8a also shows a clear rough surface.



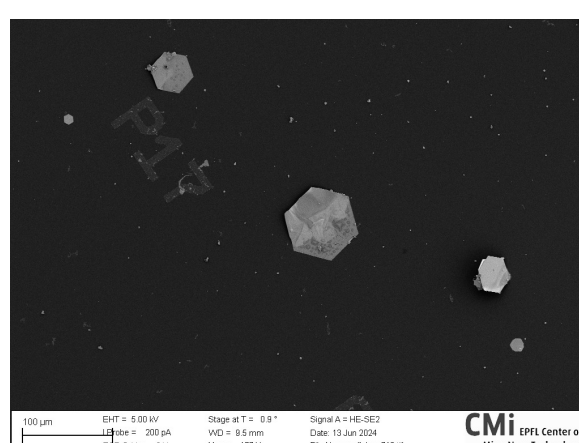
(a) SEM Image of a 60 μm diameter flake, showing surface imperfections



(b) Triangular nanoparticles contamination on the flake's surface



(a) SEM Image of an 80 μm diameter flake, showing high surface roughness



(b) Top view of the flake on a gridded substrate

3.5 Surface Stabilizing Agents and Seeded Growth

Based on the results presented earlier, I implemented the conclusions in subsequent experiments. However, both techniques yielded unsuccessful outcomes. Specifically, concerning the Citrate

ligand, the solution prepared with the earlier mentioned 0.7 ratio appears grey and lacks any plate-like formations. This suggests that the concentration of Citrate may be too high for optimal flake growth.

Additionally, I attempted to introduce Citrate when the plates reached at least 10 μm in size, using a ratio of 1:100 and 1:1000. However, this approach also did not yield satisfactory results, as there were few flakes observed. This could potentially be attributed to Citrate's role in stabilizing nanoparticles right from the beginning of the reaction, which hinders the formation of flakes.

Regarding Potassium Chloride (KCl), I tested concentrations of 30 mM, 3 mM, and 0.3 mM, added at different stages of the reaction —beginning, middle, and end of the process — to eliminate any time-related correlations, and stabilizing from the beginning. However, none of the tested concentrations of KCl showed significant improvement in the outcomes. The results did not demonstrate clear enhancements in flake growth or quality across the varying concentrations and timing of addition.

Furthermore, seeded growth proved unsuccessful due to the rapid nature of the reaction, resulting in nuclei that were too large as anticipated. Additionally, since the supersaturation monitoring method yielded similar results but with greater ease, there was no incentive to continue pursuing this direction.

4 Conclusion

The optimization of silver micro-flake fabrication through colloidal growth has been a multifaceted process, involving careful consideration of various parameters such as concentration, temperature, reaction time, and the sequence of reactant addition. Key findings from this research include:

Basic Variables Optimization: The experiments showed that higher initial concentrations of AgNO_3 and Metol facilitated rapid growth, resulting in larger flakes initially. However, beyond a certain concentration threshold, smaller particles began to dominate. Optimal conditions were identified with a concentration of 9 mM for both reactants. Room temperature was found to be ideal; lower temperatures slowed the reaction excessively, while higher temperatures increased nucleation sites, leading to smaller flakes. Although extended reaction times were hypothesized to enhance flake growth, the results revealed that prolonged reactions caused aggregation and settling of the flakes. Gentle stirring emerged as a critical factor in preventing flake aggregation.

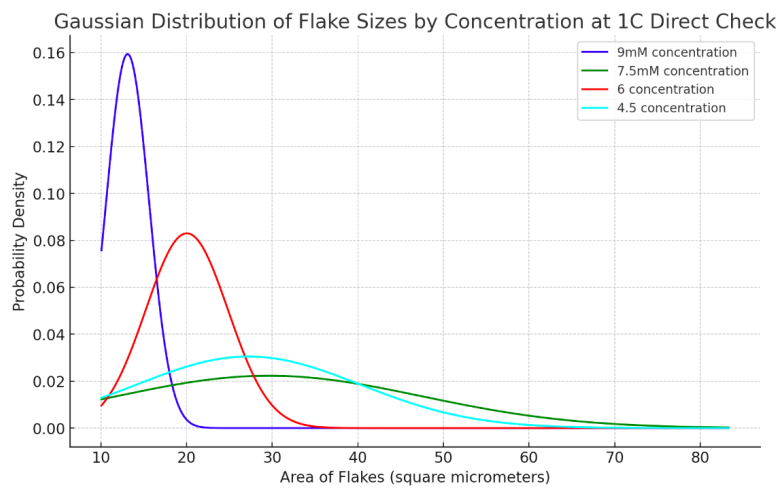
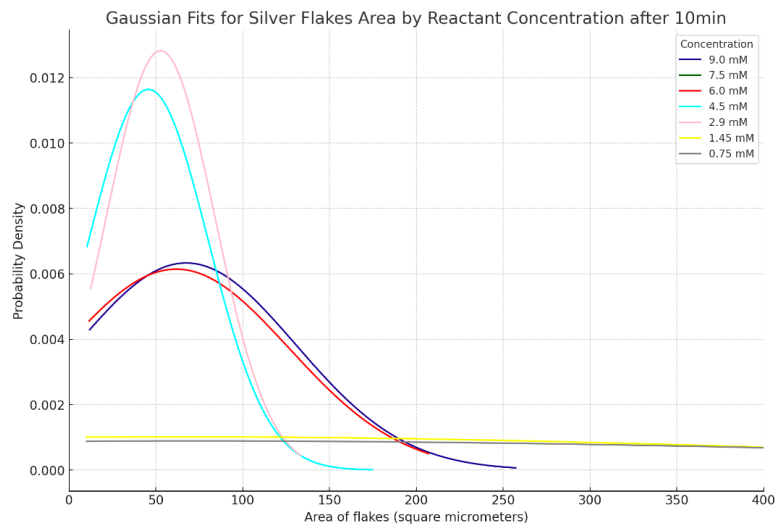
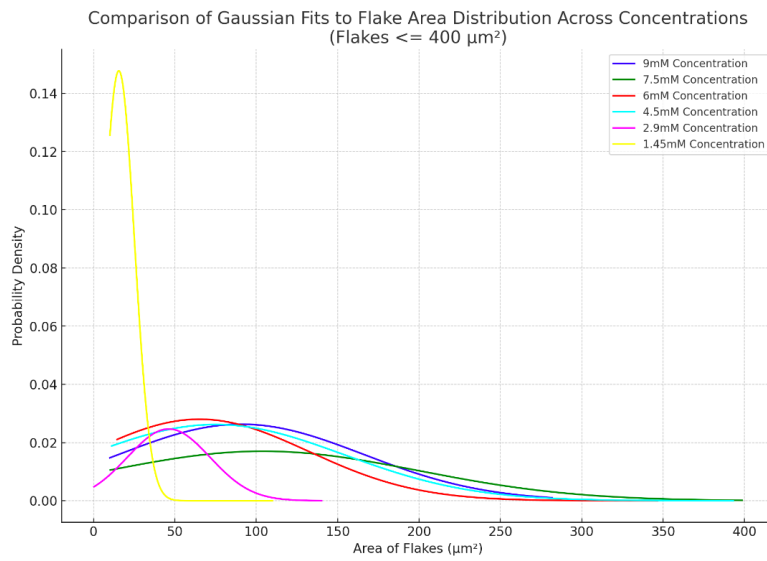
Advanced Variables Optimization: Gradually adding Metol to the AgNO_3 solution was highly effective in controlling nucleation and promoting the growth of large silver flakes. The use of stabilizing agents such as Citrate and KCl did not yield significant improvements in flake growth or quality. Seeded growth techniques also proved challenging due to the rapid nature of the AgNO_3 - Metol reaction.

My primary focus on this project was to increase the flakes' sizes and prevent contamination, such as overlapping and aggregation of particles or flakes. However, a high surface quality is crucial to minimize losses in SPP propagation, and remains an area for further improvement and exploration.

References

- [1] Fatemeh Kiani and Giulia Tagliabue. “High Aspect Ratio Au Microflakes via Gap-Assisted Synthesis”. In: *Chemistry of Materials* 34.3 (2022), pp. 1278–1288. DOI: 10.1021/acs.chemmater.1c03908. eprint: <https://doi.org/10.1021/acs.chemmater.1c03908>. URL: <https://doi.org/10.1021/acs.chemmater.1c03908>.
- [2] Dimitar Lyutov et al. “Synthesis and structure of large single crystalline silver hexagonal microplates suitable for micromachining”. In: *Materials Chemistry and Physics* 143 (Oct. 2014), pp. 642–646. DOI: 10.1016/j.matchemphys.2013.09.047.
- [3] Michel Nasilowski et al. “Two-Dimensional Colloidal Nanocrystals”. In: *Chemical Reviews* 116.18 (2016). PMID: 27434678, pp. 10934–10982. DOI: 10.1021/acs.chemrev.6b00164. eprint: <https://doi.org/10.1021/acs.chemrev.6b00164>. URL: <https://doi.org/10.1021/acs.chemrev.6b00164>.
- [4] Isabel Pastoriza-Santos and Luis Liz-Marzán. “Colloidal Silver Nanoplates: State of the Art and Future Challenges*”. In: Apr. 2020, pp. 159–195. ISBN: 9780429295188. DOI: 10.1201/9780429295188-5.
- [5] Leonardo Scarabelli et al. “Plate-Like Colloidal Metal Nanoparticles”. In: *Chemical Reviews* 123.7 (2023). PMID: 36948214, pp. 3493–3542. DOI: 10.1021/acs.chemrev.3c00033. eprint: <https://doi.org/10.1021/acs.chemrev.3c00033>. URL: <https://doi.org/10.1021/acs.chemrev.3c00033>.
- [6] Chun-Yuan Wang et al. “Giant colloidal silver crystals for low-loss linear and nonlinear plasmonics”. In: *Nature communications* 6 (July 2015), p. 7734. DOI: 10.1038/ncomms8734.
- [7] P.R. West et al. “Searching for better plasmonic materials”. In: *Laser & Photonics Reviews* 4.6 (2010), pp. 795–808. DOI: <https://doi.org/10.1002/lpor.200900055>. eprint: <https://onlinelibrary.wiley.com/doi/pdf/10.1002/lpor.200900055>. URL: <https://onlinelibrary.wiley.com/doi/abs/10.1002/lpor.200900055>.
- [8] Qiao Zhang et al. “A Systematic Study of the Synthesis of Silver Nanoplates: Is Citrate a “Magic” Reagent?” In: *Journal of the American Chemical Society* 133.46 (2011). PMID: 21999679, pp. 18931–18939. DOI: 10.1021/ja2080345. eprint: <https://doi.org/10.1021/ja2080345>. URL: <https://doi.org/10.1021/ja2080345>.
- [9] Qiao Zhang et al. “Seeded Growth of Uniform Ag Nanoplates with High Aspect Ratio and Widely Tunable Surface Plasmon Bands”. In: *Nano Letters* 10.12 (2010). PMID: 21038884, pp. 5037–5042. DOI: 10.1021/nl1032233. eprint: <https://doi.org/10.1021/nl1032233>. URL: <https://doi.org/10.1021/nl1032233>.
- [10] Tingting Zhang et al. “Controlled Multichannel Surface Plasmon Polaritons Transmission on Atomic Smooth Silver Triangular Waveguide”. In: *Advanced Optical Materials* 7 (Aug. 2019). DOI: 10.1002/adom.201900930.

5 Appendices



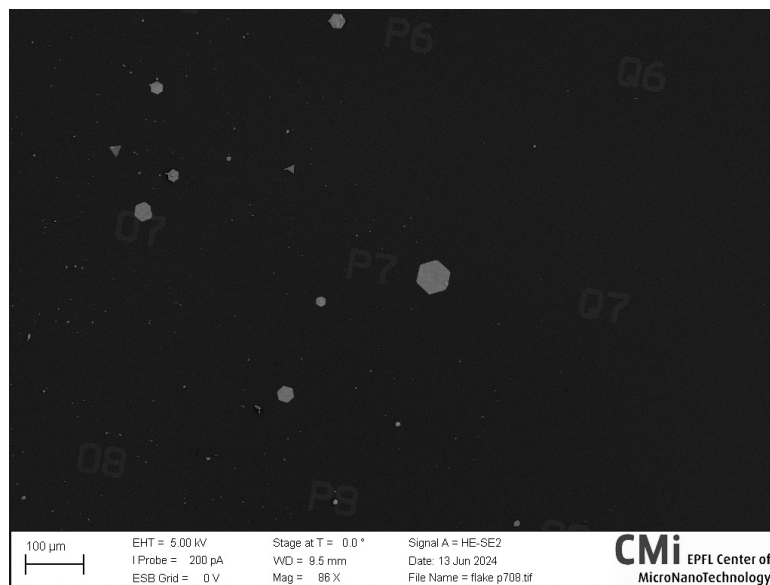
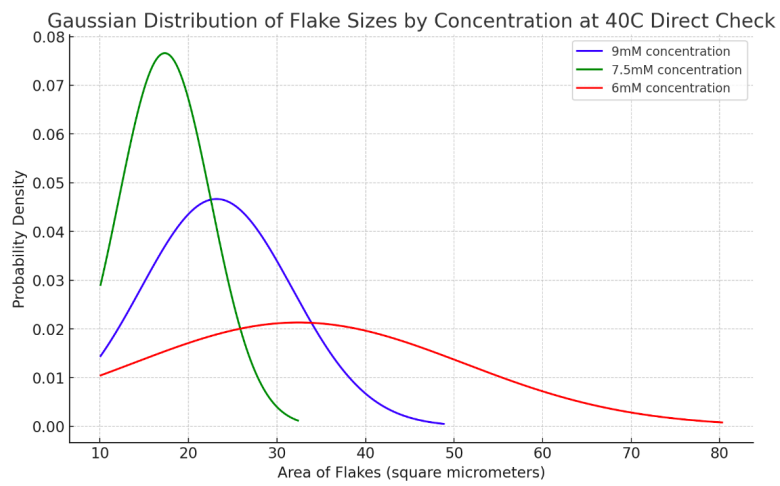


Figure 9: SEM Top View of P7 Flake



Figure 10: Optical Microscope Image of a Triangular Flake Fabricated with Supersaturation Monitoring